mathematics

MDPI

Article

Turbulent Heat Transfer Augmentation in a Square Channel by Augmenting the Flow Pattern with Novel Arc-Shaped Ribs

Basma Souayeh [1,2,*] and Suvanjan Bhattacharyya [3]

[1] Department of Physics, College of Science, King Faisal University, P.O. Box 400, Al-Ahsa 31982, Saudi Arabia
[2] Laboratory of Fluid Mechanics, Physics Department, Faculty of Sciences of Tunis, University of Tunis El Manar, Tunis 2092, Tunisia
[3] Department of Mechanical Engineering, Birla Institute of Technology and Science Pilani, Pilani Campus, Vidya Vihar, Pilani 333031, Rajasthan, India
* Correspondence: bsouayeh@kfu.edu.sa or basma.souayeh@gmail.com

Abstract: Solar water heaters (SWHs) are widely used in HVAC industries as well as in households for different heating purposes. The present numerical simulation focuses on the investigation of the thermo-hydraulic performance of novel semi-arc-rib SWHs. Semi-arc-shaped ribs in the square channel of the absorber plates with different pitch and height ratios are investigated in this study. The present novel modification disturbs the boundary layers by generating vortices, and thus, enhanced fluid mixing takes place. Water with a Reynolds number (Re) ranging from 4000 to 25,000 is used as a working fluid, and a 1.0 kW/m^2 heat flux is imposed on the tube wall. The results demonstrate a significant increase in the Nusselt number (Nu) as the fluid layers localize behind each rib near the absorber plates, and at the same time, the number of swirls generated inside the tube and the frictional losses both increased noticeably. To ensure the effectivity of the present novel SWH geometry, the thermo-hydraulic performance (η) for each case was calculated, and it was found that in all the cases, it was greater than unity, which signifies that the present semi-arc-rib SWH is promising and can be used in HVAC industrial and household applications.

Keywords: solar water heater; semi-circular arc; heat transfer; enhancement; swirl flow; thermal performance

MSC: 76-10

Citation: Souayeh, B.; Bhattacharyya, S. Turbulent Heat Transfer Augmentation in a Square Channel by Augmenting the Flow Pattern with Novel Arc-Shaped Ribs. *Mathematics* **2023**, *11*, 1490. https://doi.org/10.3390/math11061490

Academic Editor: Ramoshweu Solomon Lebelo

Received: 8 January 2023
Revised: 28 February 2023
Accepted: 9 March 2023
Published: 18 March 2023

1. Introduction

Energy consumption has increased as a result of welfare development and ongoing population rise across the world. Energy efficiency and sustainability are becoming more significant in today's world as a result of a supply and demand imbalance. Therefore, a significant amount of effort is being made to develop energy-efficient devices without any major financial investment.

A solar water heater is an important device that uses solar energy to heat water for domestic or commercial use. It consists of a solar collector, which absorbs the sun's energy, and a storage tank for hot water. The solar collector can be flat plate or evacuated tube and is typically mounted on a roof or a wall facing the sun. The storage tank is typically located near the collector and is insulated to reduce heat loss. The hot water produced by the solar collector is transferred to the storage tank, where it can be used as needed. Solar water heaters are an environmentally friendly and cost-effective alternative to traditional water heating systems that rely on fossil fuels.

Heat transfer enhancement for a solar water heater refers to methods used to improve the heat transfer rate from the solar collector to the water in the storage tank. This can be achieved by increasing the heat transfer area, the heat transfer coefficient, or the temperature

difference between the two fluids. The common method for heat transfer enhancement is to improve the design of the solar collector by incorporating fins or other structures to increase the heat transfer area and, at the same time, use more thermally conductive fluids, such as water, with a high thermal conductivity, which can be used to transfer heat more efficiently. Implementing these heat transfer enhancement methods can lead to an improved performance and increased efficiency of a solar water heater. Generally, the technique of heat transfer enhancement (HTE) is divided into three categories: active techniques [1]; passive techniques [2,3]; and combined or combinational techniques [4,5]. Conventional heat exchangers (HEs) are incapable of satisfying the demand of heating and cooling in modern industries with their limited capacity. Modifications are being applied to the heat exchangers to enhance their thermal and flow performance. This includes use of ribs, turbulators, ultrasound, vibrations, magnetic field, electric field, advance heat transfer fluids, etc. [6]. The objective is to increase the thermohydraulic performance of a thermal device, whether by increasing the surface area for fluid interaction, by increasing the swirling motion of the fluid, or by increasing the thermal conductivity of the fluid. The thermohydraulic performance of a heat exchanger refers to its ability to transfer heat from one fluid to another. This performance is influenced by various factors, such as the temperature difference between the two fluids, the flow rate of the fluids, the heat transfer area, and the heat transfer coefficient. The overall thermohydraulic performance can be evaluated by calculating the heat transfer rate, the thermal efficiency, and the pressure drop across the heat exchanger. Improving the thermohydraulic performance of a heat exchanger can be achieved by optimizing these factors and increasing the heat transfer area and the heat transfer coefficient.

Among the various techniques of HTE in SWHs, ribs are the simplest, and the enhancement is appreciable when compared with other methods [7–10]. Deo et al. [8] experimentally investigated the influence of staggered inclined ribs on the thermal and flow performance of solar air heaters and reported significant enhancements in the performance and efficiency of solar air heaters (SAHs) when compared with a plane channel. Zhang et al. [9] studied the effect of longitudinal intersecting ribs on the thermohydraulic performance of gas turbine blades and reported an increase in the overall efficiency. Singh and Ekkad [11] reported on the implementation of ribs, along with dimples, for improving the cooling performance of gas turbine blades. It has been noted that the presence of both ribs and dimples enhanced the heat transfer (HT) and improved thermal hydraulic performance. Yang et al. [12] carried out a simulation study to study the impacts of high-blockage ribs on the HT and pressure drop (PD) characteristics of gas turbine blades. It was reported that the HT coefficient increases with an increase in the Re, the rib space to height ratio, and area of the ribbed portion covered in the channel. Alfarawi et al. [13] experimentally evaluated the thermal and hydrodynamic characteristics of air inside a rectangular ribbed channel. Tanda [14] presented performance results of SAHs fitted with four sets of ribs and found significant enhancements in the HT as well as the PD. Kumar et al. [15] reported on multiple arc-shaped ribs for SAHs, and although changing the roughness parameters resulted in an increase in the solar air heater's pumping power, there was a notable improvement in the thermal performance of the device. Hans et al. [16] examined single discrete arc ribs and how they affected SAH performance with constant parameter values. In single arc (discrete) ribs, the Nu was improved by 2.63 times more than the smooth SAH. Promvonge [17] experimentally reported on the influences of quadruple-twisted tapes arranged in four different combinations and V-fins on the HT and PD performance of square HE ducts. The V-finned counter-twisted tape had a much better thermal performance than the quadruple-twisted tapes. Mokkapati and Lin [18] reported on the thermohydraulic performance of corrugated tube HE tubes fitted with twisted tapes. The findings indicate that, as compared to plain tubes and corrugated tube HEs without twisted tapes, annularly corrugated tube heat exchangers with twisted tape boost the rate of HT by about 235.3% and 67.26%, respectively. Abraham and Vedula [19] investigated straight, V-shaped, and W-shaped ribs with apex angles of 45°. The ribs' height was kept as constant, and the pitch

was varied. It was reported that the variation in the Nu ratios for the V and W configurations was negligible for the same pumping capacity. Chung et al. [20] reported on simple square ribs placed at a 60^{o} angle in line with the direction of flow. They compared the performance of inclined ribs with that of intersecting ribs. The aspect ratio of the channel was varied between 1 and 4. It was found that the presence of intersecting ribs aided in the generation of more vortices, which resulted in a higher heat transfer enhancement for all the aspect ratios. Gawande et al. [7] employed L-shaped ribs for HTE in SAHs. The dimensions of the ribs remained constant, and the pitch or gap between the ribs varied from 10 to 25 mm. Configuration with a higher pitch ratio resulted in higher augmentation. Liu et al. [21] numerically investigated perforated square ribs for cooling channel application. The ribs under investigation were perforated with square and circular holes. It was reported that the perforated ribs showed an enhanced thermal performance when compared with non-perforated ribs and were suitable for cooling application. Bhattacharyya et al. [22] investigated alternating inclined ribs for their thermohydraulic performance in a circular channel. Four angles of attack were investigated for a wide range of Re values, covering laminar, transition, and turbulent flow regimes.

2. Objective

The use of novel arc-shaped ribs as a means of enhancing heat transfer is a new technique in the field of HTE. Arc-shaped ribs are small devices that are attached to the surface of a heat exchanger wall and cause the fluid flow to become turbulent, which can enhance the convective heat transfer and improve the overall heat transfer coefficient. From the literature, it was found that many researchers are working on circular tubes to enhance heat transfer by inserting only unidirectional ribs, and it was also noticed that in many cases, the thermo-hydraulic performance of the system falls below unity. As per the authors' knowledge, thus far, no research has been conducted on square channels with semi-arc-shaped ribs on four sides of the channel to enhance HT. Overall, the use of ribs for heat transfer enhancement remains an active area of research and development, with a significant degree of novelty and potential for continued innovation. In this study, a turbulent HTE in the square channel with the augmentation of the flow pattern using novel arc-shaped ribs in SWHs is presented.

3. Computational Domain, Boundary Conditions and Meshing

The dimensions of the 3D square channel are 20 mm $\times$ 20 mm, and a length of 2500 mm is taken for the present computational investigation; these dimensions are constant throughout the study. To enhance the convective HT rate, semi-arc ribs are attached to the SWH walls. The computational domain is shown in Figure 1. The current study concerns the region of the turbulent flow regime with a high Re ranging from 4000 to 25,000. A fully developed velocity profile is incorporated at the SWH inlet for different Re values. All side walls are assumed to have iso-heat flux boundary conditions with 1.0 kW/m^2 throughout the test section. Table 1 presents the tested parameters. To make efficient use of the computer resources, simulations were conducted based on the assumptions below:

- The flow is incompressible, and steady-state equations are solved to predict the results.
- The air travels easily over the solid surface with a no-slip boundary condition.
- In ambient circumstances, water as the working fluid, enters in the computational domain.

Table 1. Computational Parameters.

Parameter	Range
Inner diameter of the tube, D	20 mm
Height ratio, d/D = H	0.5, 0.4, 0.25
Pitch ratio, p/D = s	1, 1.5, 2.0
Reynolds number (Re)	4000–25,000

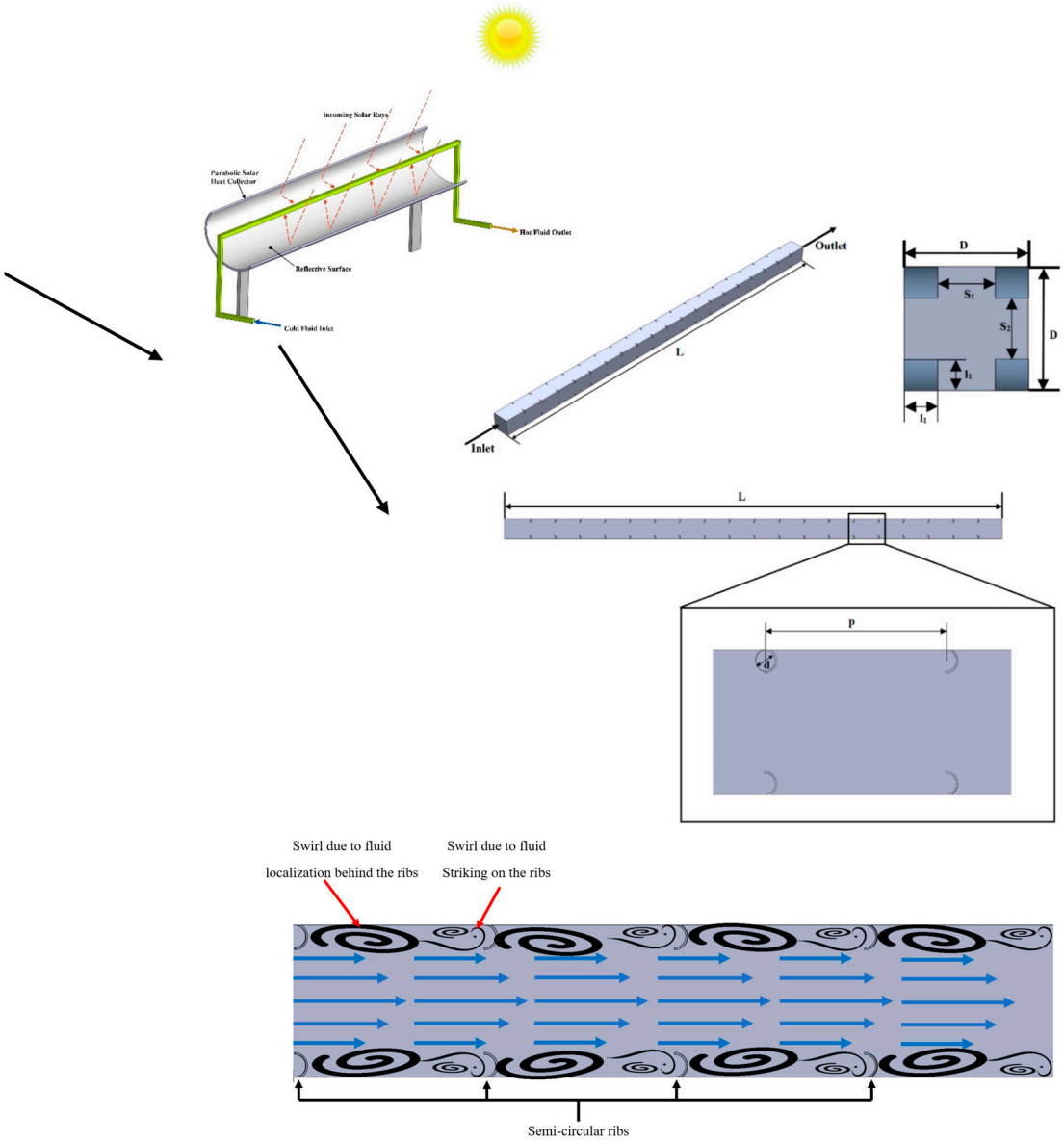

Figure 1. Computational domain.

The steady incompressible viscous flow is computationally simulated using a modified SWH with semi-arc cross-sectional roughness elements. The roughness elements are positioned on each corner of the square channel. The flow field and HT through the SWH are governed by the Navier–Stokes equation and the energy equation, which are written as follows [22]:

$$\frac{\partial}{\partial x_i}(\rho \bar{u}_i) = 0 \tag{1}$$

$$\frac{\partial}{\partial x_i}(\rho \bar{u}_i \bar{u}_j) + \frac{\partial}{\partial x_i}\bar{P}' \frac{\partial}{\partial x_i}\left[(\mu + \mu_t)\left(\frac{\partial}{\partial x_j}\bar{u}_i + \frac{\partial}{\partial x_i}\bar{u}_j\right)\right] \tag{2}$$

$$C_P\left[\bar{u}_i \frac{\partial}{\partial x_i}(rho\bar{T}) + \frac{\partial}{\partial x_i}\left(\frac{\mu_t}{\mathrm{Pr}_t} \times \frac{\partial}{\partial x_i}\bar{T}\right)\right] = \frac{\partial}{\partial x_i}\left(\lambda \times \frac{\partial}{\partial x_i}\bar{T}\right) \tag{3}$$

The variables P, u, and T in the equation above represent pressure, velocity, and temperature, respectively.

The important RANS turbulent model, using the k-ω RNG model, is implemented because this model includes an additional ω-equation that improves the accuracy of the projected results. This model includes the following equation:

$$\frac{\partial(\rho k u_i)}{\partial x_i} - \frac{\partial}{\partial x_j}\left(\alpha_k \mu_{eff} \frac{\partial k}{\partial x_j}\right) - G_k + \rho\varepsilon = 0 \tag{4}$$

$$\frac{\partial(\rho \varepsilon u_i)}{\partial x_i} - \frac{\partial}{\partial x_j}\left(\alpha_\varepsilon \mu_{eff} \frac{\partial \varepsilon}{\partial x_j}\right) - \frac{C_{1'\varepsilon}}{k} G_k + C_2 \rho \frac{\varepsilon^2}{k} = R_\varepsilon \tag{5}$$

$$\mu_{eff} = \mu_f + \mu_t = \mu_f + \rho C_\mu \frac{k^2}{\varepsilon} \tag{6}$$

The simulation software ANSYS Fluent 18.1 is used to simulate the HT and PD characteristics in the modified SWH with semi arc-shaped ribs. To discretize, the governing equations, second-order numeric techniques are used to improve the accuracy and reduce literation errors. In addition, the convergence threshold for the continuity and momentum components is established as 10^{-6}, and for the energy equation, it is 10^{-8} [22]. Steady-state calculations are performed on the quantities required to estimate the thermal–hydraulic performance.

In the test section, all the properties such as the velocity, pressure, temperature, etc., are measured under steady-state conditions. The tetrahedral element is formed in the semi-arc-shape-ribbed SWH. The Y+ value is kept as smaller than one for the rib roughness and the heated wall. ANSYS ICEM is used to construct the meshing, and the values of all the meshed elements are guaranteed to be more than 0.75. The procedure of constructing the mesh begins with 10 mm-sized coarse components, and the process is continued until the results have no or minimal influence on the mesh refinement (or element size). The meshing is shown in Figure 2, and Table 2 presents the specifics of the grid refinement along with the appropriate solution for the average Nu and friction factor (f). As a result, the grid of 2,987,675 nodes, which is grid 1 in Table 1, is used for all the simulations in order to save computational time and resources.

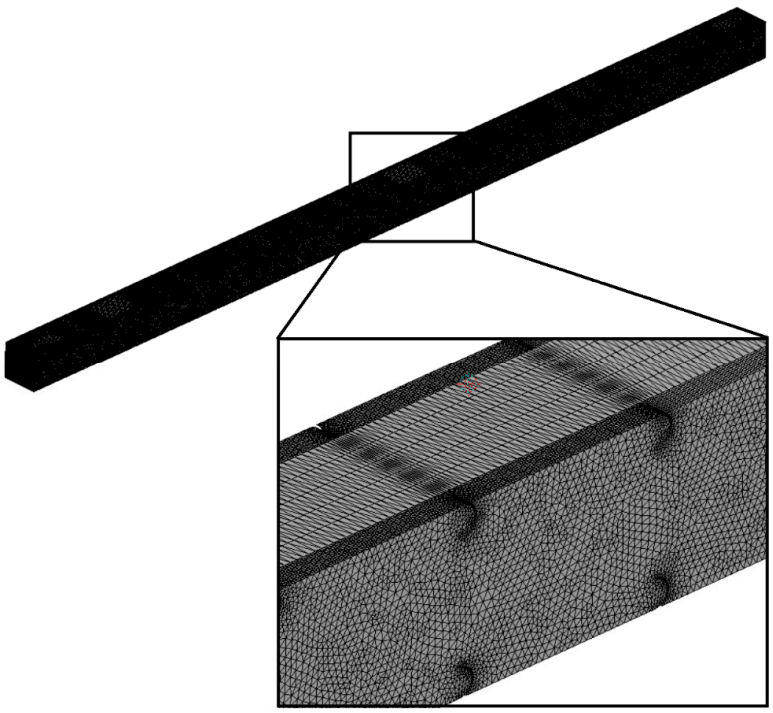

Figure 2. Meshing of the computational domain.

Table 2. Grid independence test.

	Nodes	Nu	f	η
Re = 10,000, Semi-Arc-Shaped Rib, P = 1.0, H = 0.5				
Grid 1	2,987,675	132.370	0.037	1.455
Grid 2	3,345,789	132.373	0.037	1.455
Grid 3	3,876,444	132.391	0.038	1.456

Heat transport to the working fluid is quantified using the first law written below. It is known from the first law of thermodynamics that the rate of net HT to the working fluid is proportional to the temperature difference between the inlet and outlet fluids, as well as the mass flow rate and specific heat of the induced fluid [3,23].

$$Q = mc_p(T_o - T_i) \tag{7}$$

The heat transfer coefficient is calculated using the following equation, as stated by Bhattacharyya et al. [3]:

$$h = \frac{q_w}{T_w - T_b} \tag{8}$$

The Nusselt number measures the extent to which convection contributes to the total heat transfer relative to conduction. A comparison of the superiority of convective heat transfer vs. conductive heat transfer may be conducted using this dimensionless metric. In other words, a rising Nu value suggests that convection is a more important heat transfer mechanism than conduction. One possible expression of this is [23]:

$$Nu_{avg} = \frac{hD}{k} \tag{9}$$

where k is the thermal conductivity of the material.

One of the most critical parameters for assessment is known as Darcy's Friction Factor. This parameter is indicated by f and may be determined using the formula listed below [22]:

$$f = \frac{\Delta \mathrm{P}}{\frac{\mathrm{L}}{\mathrm{D}} \frac{1}{2} \rho \mathrm{V}^2} \tag{10}$$

Here, ρ, D, and L signify the density of the fluid, hydraulic diameter, and length of the SAH, respectively. Based on the free cross-section of an insert, the bulk fluid velocity and the static pressure drop are both designated by the ΔP. Reynolds number is used to compute the velocity of the working fluid (Re). The formula is as follows [3]:

$$Re = \frac{\rho V D}{\mu} \tag{11}$$

The increment in Nu_{avg} and f due to the semi-arc-shaped ribs' imposition on the SAHs, with respect to smooth SAHs, is determined by Nu_c and f_c, where $\mathrm{Nu_c}$ and $\mathrm{f_c}$ can be determined as [22]:

$$Nu_{\mathrm{c}} = \frac{Nu_{\mathrm{avg}}\big|_{\text{with rib}}}{Nu_{\mathrm{avg}}\big|_{\text{smooth}}} \tag{12}$$

$$f_c = \frac{f|_{\text{with rib}}}{f|_{\text{smooth}}} \tag{13}$$

From Equations (12) and (13), the thermo-hydraulic performance (THP) can be determined as [22]:

$$THP = Nu_{\mathrm{c}} \times f_c^{-\frac{1}{3}} \tag{14}$$

4. Validation

It is essential to validate the present simulations with the literature. The Nusselt numbers for plain channels obtained by simulation are compared in Figure 3a with those from Dittus–Boelter [23]. Figure 3b contrasts the friction factor with the historically reliable Blasius correlation [24]. The average absolute variance for the Nusselt number was found to be 4.0% and the average deviation for the friction factor was found to be 2.0% when comparing the simulated findings with the projected data. The current computational model can be used to calculate the flow and HT in a square channel with semi-arc-shaped ribs if the simulation accuracy is accepted.

$$Nu = 0.0023\mathrm{Re}^{0.8}\mathrm{Pr}^{0.4} \tag{15}$$

$$f = \frac{0.316}{Re^{\frac{1}{4}}} \tag{16}$$

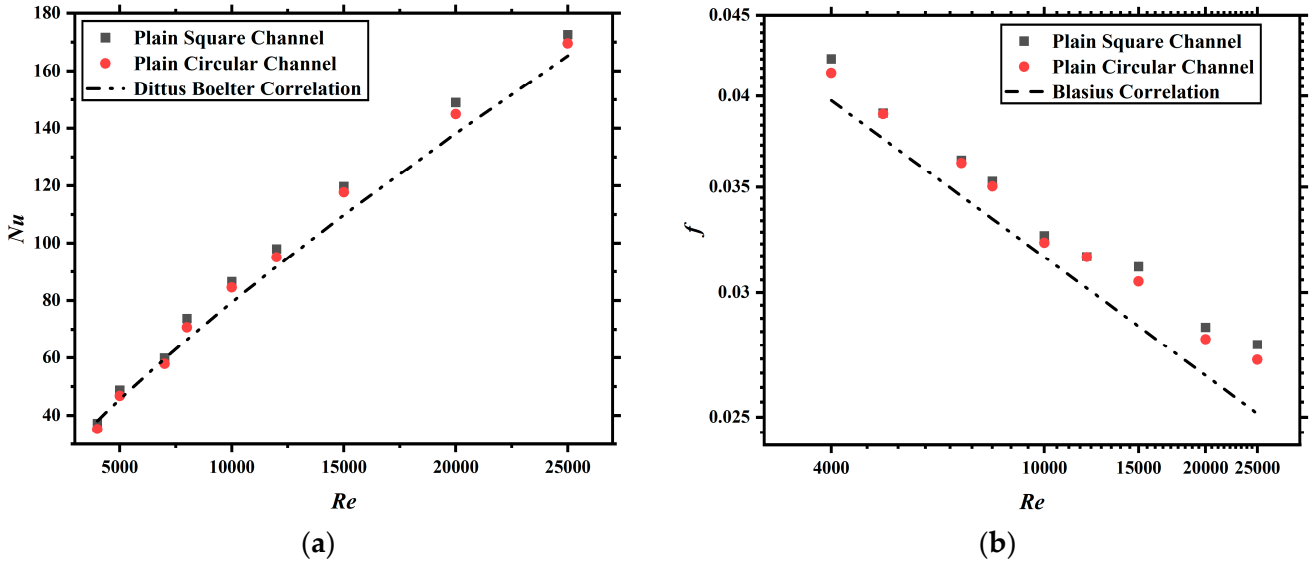

Figure 3. Validation of the computation study: (**a**) *Nu* and (**b**) *f*.

5. Results and Discussion

This important discussion section provides a detailed summary of the present computation investigation on the novel semi-arc-shaped ribs. Semi arc-shaped ribs are mainly responsible for disturbing the hydrodynamic and thermal boundary layers of the water flow, which leads to the formation of vortices near the heated walls and better mixing of the fluid layers. Due to the above-mentioned phenomenon, convective heat transfer is superior to conductive heat transfer. The current study concerns turbulent flow with Re ranging from 4000 to 25,000. Heat transfer, pressure drop, the j-factor, Bejan number, and thermo-hydraulic performance, as a function of the Re results, are discussed in this section.

Heat transfer in SWH was enhanced significantly by the incorporation of semi-arc-shaped ribs inside the square tube, as shown in Figure 4a. A decrease in the conduction HT and an increase in the convection HT occur when ribs are added to the SWH walls, and this is because the ribs increase the convective surface area. In addition, the development of the boundary layer acts as a fence for the HT, as this is a forced convection heat transfer scenario, and, as a result, the ribs installed in the flow field aid in the disruption of the boundary layer and boost the rate of HT.

Considering three different pitch ratios (P) of the semi-arc-shaped ribs, Figure 4a shows a plot of the average Nu as a function of Re for different height and pitch ratios. Convective heat transfer coefficients increase with increasing Re or flow velocities because this type of heat transfer is driven by forced convection. Increases in flow velocity raise

the Re, which causes the flow to become more turbulent. This means that the fluid layers may be travelling over many other fluid layers, leading to greater mixing in the flow and a consequently greater heat transfer from the channel wall. The insertion of the novel-shaped ribs will increase the Nusselt number in heat transfer situations by creating turbulence in the fluid flow and enhancing the convective heat transfer. This will lead to an increase in the overall heat transfer coefficient and result in an increased Nusselt number. One can see from Figure 4a that the Nu increases uniformly with the Re for all the tested cases. In addition, when the roughness pitch ratio increases, the Nu drops for a certain Re. The ratio of the rib pitch to the rib height is the relative roughness pitch.

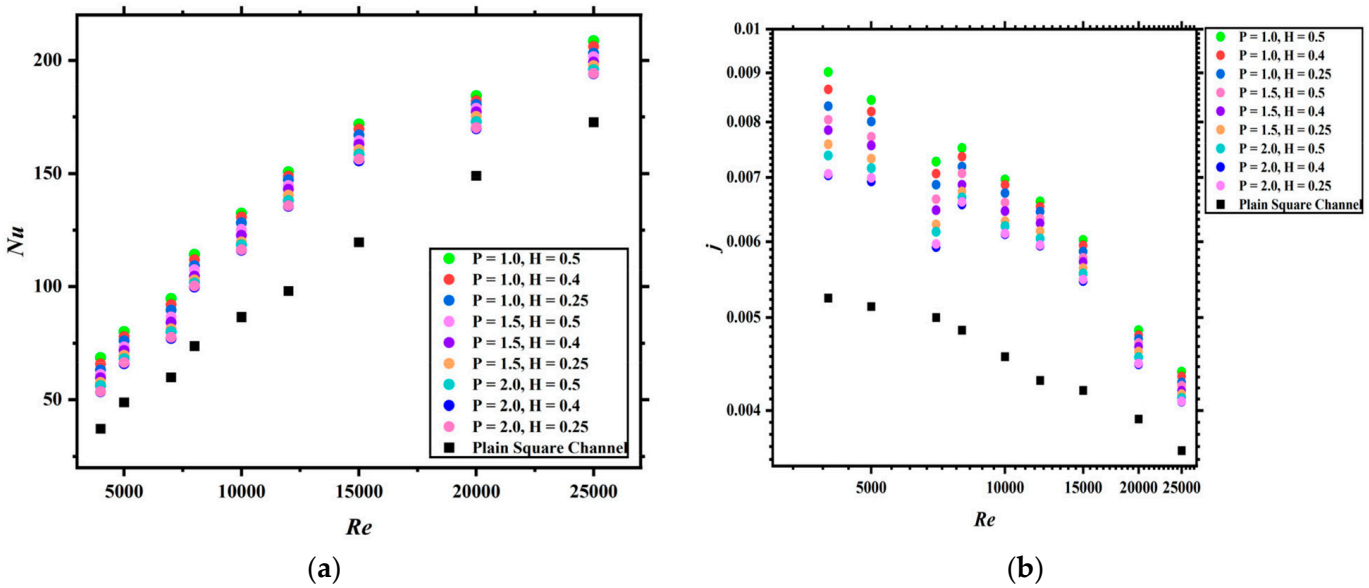

Figure 4. (**a**) Nu as a function of Re at different pitch and height ratios, and (**b**) Colburn *j-factor* as a function of Re at different pitch and height ratios.

The Colburn j-factor is a dimensionless number used in the field of HT to predict the convective HT coefficient in forced convection. It is defined as the ratio of the convective HT coefficient to the product of the fluid's dynamic viscosity, the density of the fluid, and the square of the characteristic length (L) over which the HT occurs. It is important to note that the Colburn j-factor is an empirical coefficient, meaning that it is determined experimentally and may vary depending on the specific conditions of the HT process. In Figure 4b, it is apparent that the Colburn j-factor decreases with a rise in Re. This may be due to the novel rib creating turbulence in the fluid flow, which enhances the convective heat transfer and increases the overall heat transfer coefficient. Moreover, placing rib inserts in SWHs enhances the j-factor, meaning that higher heat transfer occurs due to the better mixing of the fluid. A higher j-factor can be observed when a small pitch ratio and high height ratio of the ribs are present. However, the effect of rib insertion on the Colburn j-factor will depend on the specific configuration and the thermal–fluid properties involved.

In the presence of semi-arc-shaped ribs, there is a flow separation that can be appreciated by examining Figure 5a,b and this can lead to a breakdown of the boundary layer, as well as the reattachment of the separated boundary layer, eddy generation at the rib tips and in the inter-rib regions, and enhanced mixing owing to the development of localized turbulence. The flow is obstructed (as one can see from Figure 5a,b), the boundary layer is stunted, and the local turbulence is increased as the number of ribs is increased. This leads to a greater rate of HT.

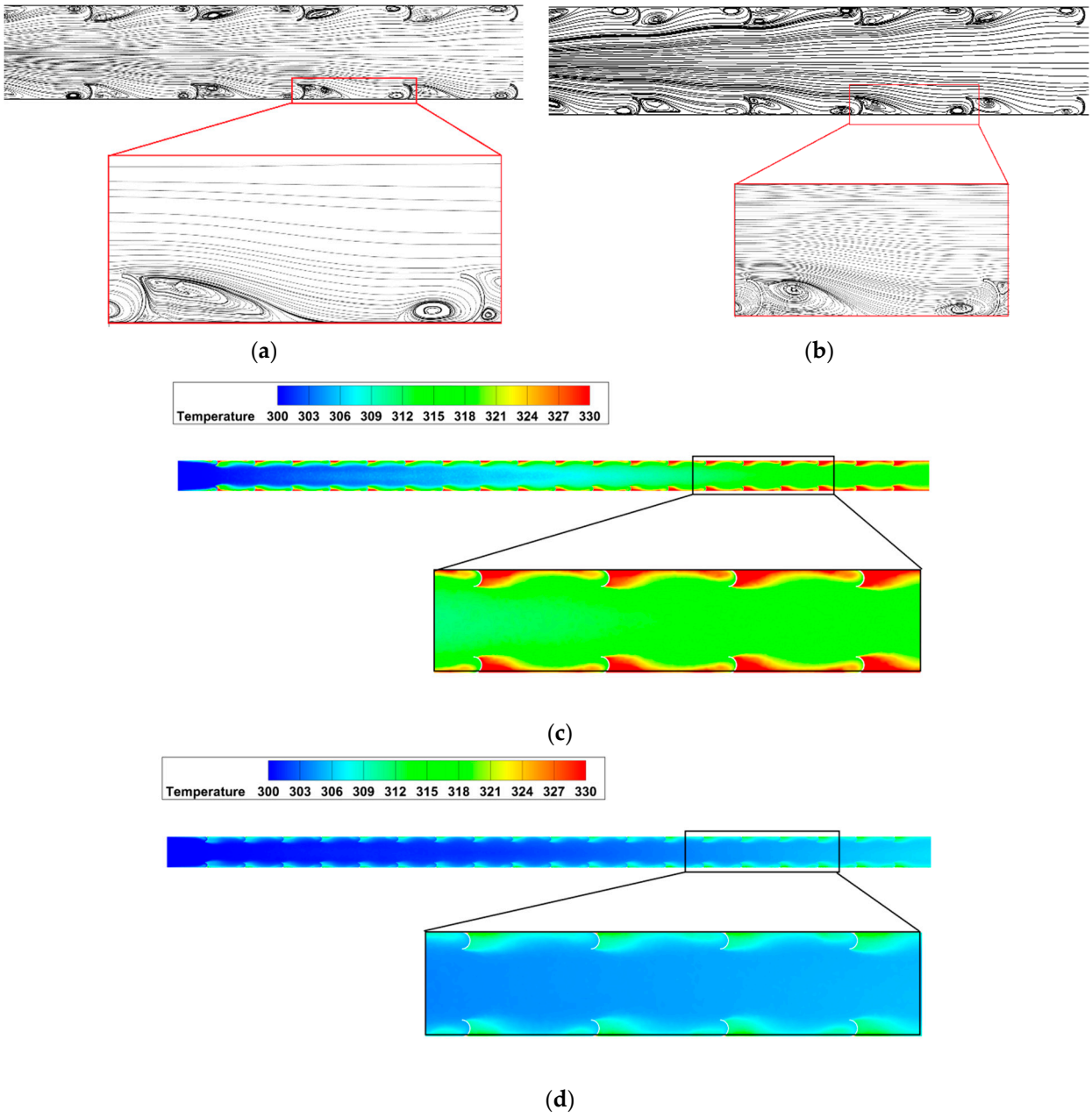

Figure 5. (**a**) Flow pattern around semi-arc-shaped ribs at Re 10,000, (**b**) flow pattern around semi-arc-shaped ribs at Re 25,000, (**c**) temperature contour around semi-arc-shaped ribs at Re 10,000, and (**d**) temperature contour around semi-arc-shaped ribs at Re 25,000.

In HT and fluid flow problems, the PD, in terms of f, is very important in order to calculate and, accordingly, understand the performance of the system. The f is a measure of the resistance to flow in a channel. It is an important factor for determining the pressure drop and flow rate in a system. In an SWH, the insertion of rib inserts can increase the friction factor by creating a more turbulent flow of water through the pipe. In the present study, it was observed that placing ribs inside the SWH increases the HT rate significantly. On the other hand, an increase in frictional loss is also observed after imposing the ribs inside the channel. Figure 6 shows that f decreases with a rise in Re. While modified SWHs are analyzed here, a noticeable increase in f is observed in comparison with smooth channel SWHs. The friction factor increases with a decrease in the pitch ratio and increase in the height ratio. A small pitch ratio signifies smaller gaps between two consecutive ribs, and the height ratio signifies the height of the ribs. From Figure 6, it is clearly apparent

that when the gaps between the ribs decrease, the friction factor increases, because in this scenario, the number of vortices is high, and due to the localization of the fluid, the friction factor increases significantly. The height of the ribs plays a significant role in creating vortices. Increases in height mainly create larger vortices, and thus, f increases with an increase in the height of the ribs.

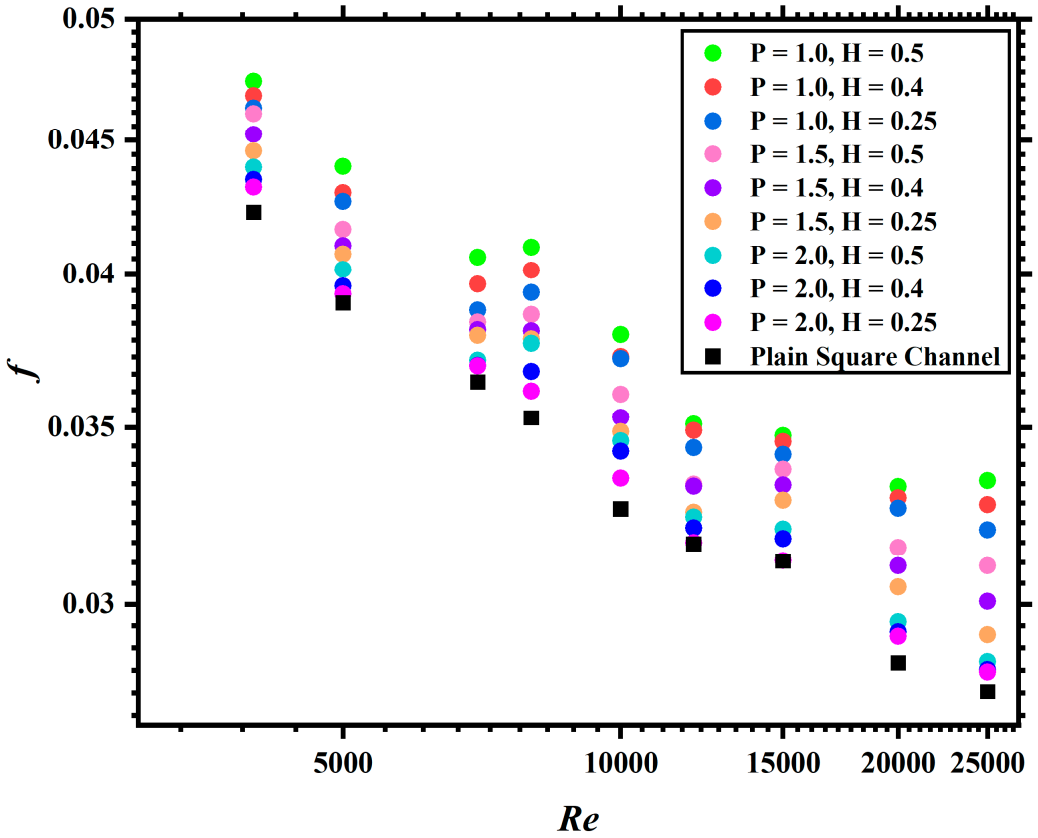

Figure 6. Friction factor as a function of Re at different pitch and height ratios.

Entropy analysis is an important aspect to study in thermal systems. The Bejan number is defined as the ratio of the system irreversibility to the total system irreversibility due to flow dynamics. It is often used to predict the flow patterns and HT characteristics of fluids in channels. The Bejan number can be used to design heat exchangers and predict the performance of heat transfer equipment. In general, a high Bejan number indicates that convective heat transfer is more important than conductive HT, while a low Bejan number indicates the opposite. The Bejan number is often used in conjunction with other dimensionless numbers, such as the Re and the Prandtl number, to predict the behavior of fluids in different flow regimes.

Generally, thermal entropy generation can be defined as [25,26]:

$$\dot{S}_{g,th} = \frac{Q_{avg}^2}{Nu\pi k T_i T_0 L} \tag{17}$$

Similarly, frictional entropy generation can be defined as [25,26]:

$$\dot{S}_{g.f} = \frac{8 f \dot{m}^3 L}{\rho^2 \pi^2 D_i^5 (T_0 - T_i)} \ln\left(\frac{T_o}{T_i}\right) \tag{18}$$

Finally, the Bejan number is defined as [26]:

$$Be = \frac{\dot{S}_{g,th}}{\dot{S}_{g,th} + \dot{S}_{g,f}} \tag{19}$$

In Figure 7, one can see that the Bejan number decreases with an increase in Re. An enhancement of the Bejan number due to the placement of the ribs was clearly observed in the present study. This signifies that the HTE is due to the placement of ribs in SWHs.

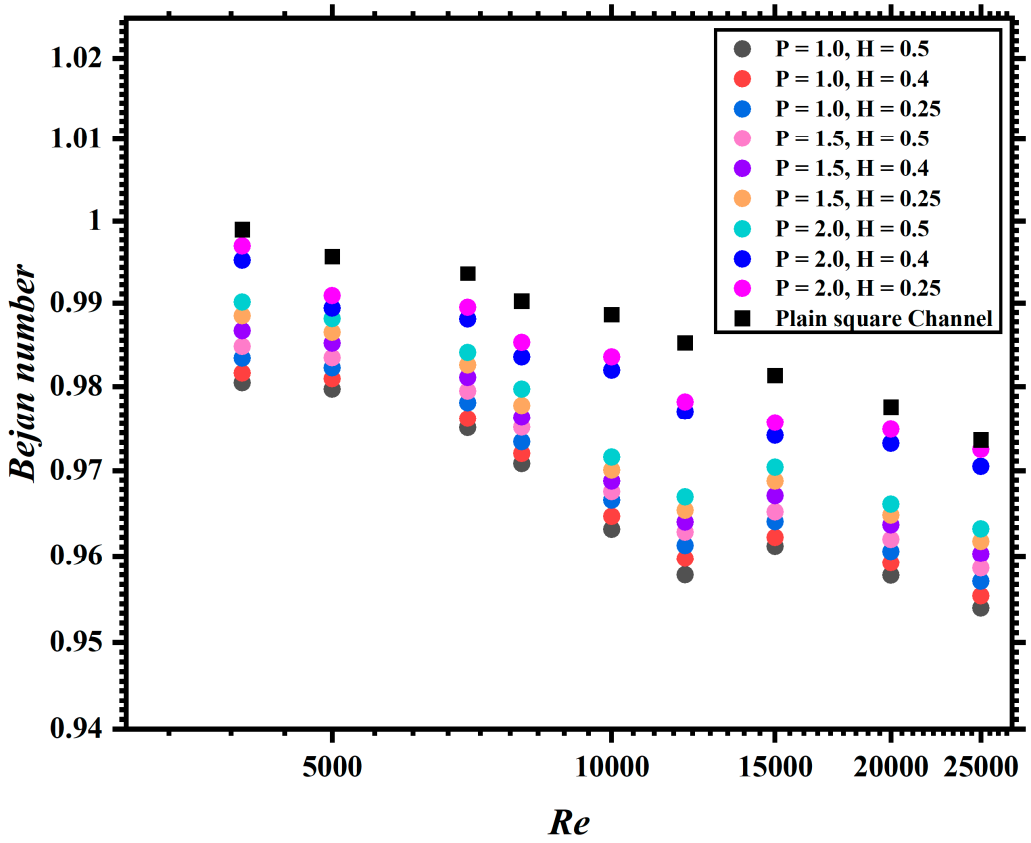

Figure 7. Bejan number (Be) as a function of Re at different pitch and height ratios.

Thermo-hydraulic performance (THP) is a parameter used to predict efficient modification in heat exchangers. THP is the ratio of Nu and f (Equation (11)). In the present study, thermo-hydraulic performance mainly signifies the effectivity of the rib inserts in SWHs. Figure 8 shows a decrease in THP with increasing Re. The placement of ribs improves the THP, which means that Nu increases higher than the increase in frictional loss. This signifies that ribs are an effective way to enhance the efficiency of SWHs. A lower pitch ratio and higher height ratio (P = 1.0, H = 0.5) perform better, as per Figure 8a. Keeping pitch ratio constant (P = 1.0), it is apparent that a higher height ratio (H = 0.5) results in higher performance increments. Similarly, when H = 0.5 is kept as constant, a lower pitch ratio (P = 1.0) results in high performance enhancement for each given height ratio. Moreover, it is important to note that for all the tested cases, the THP is greater than unity, which means that the present SWH system is promising and can be implemented.

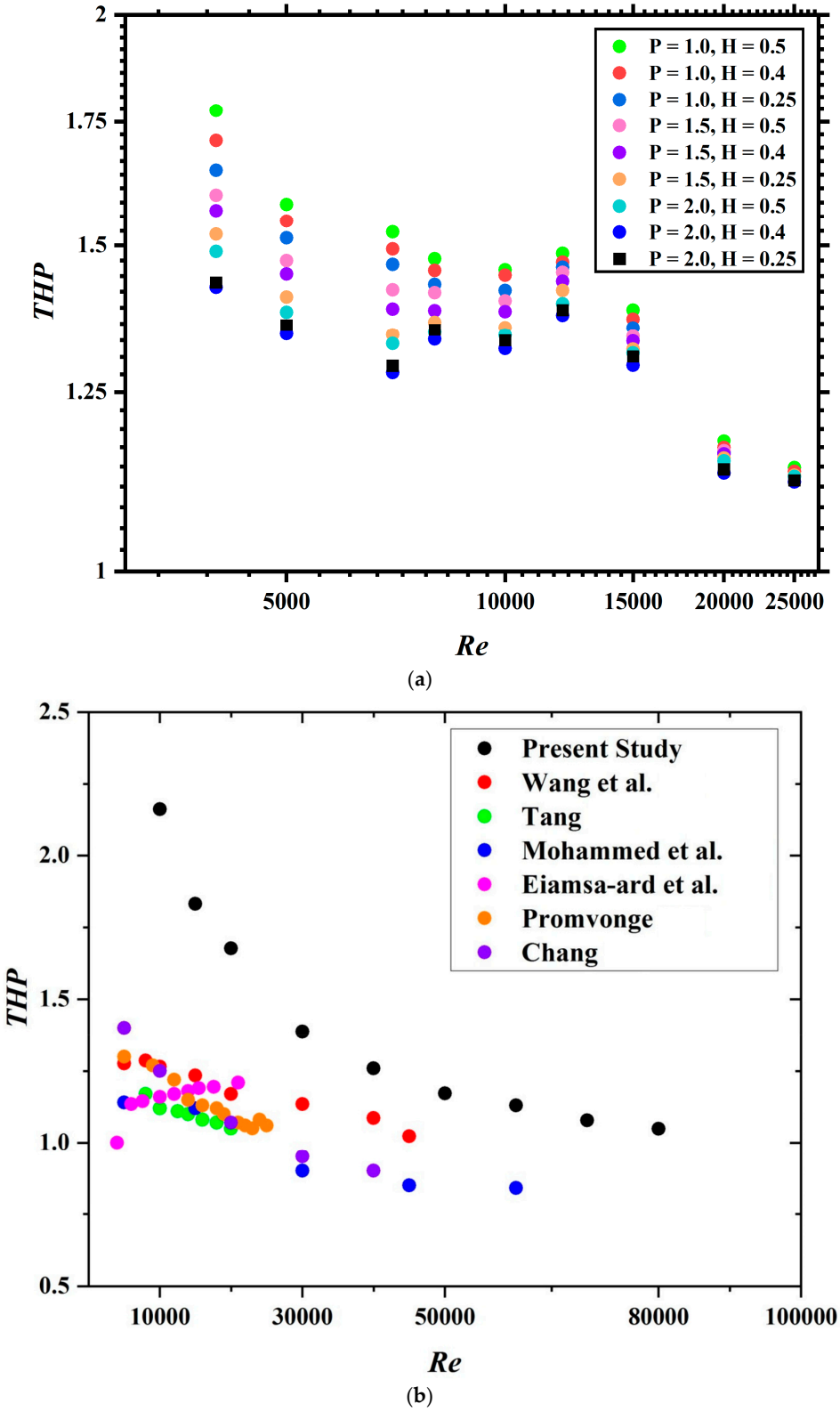

Figure 8. (**a**) Thermo-hydraulic performance varies with Re at different pitch and height ratios. (**b**) Comparison of the present study with the literature [27–32].

Figure 8b presents a comparison plot of the present study (best case: y = 0.5, h = 0.2, θ = 60°) with the literature (research in similar areas). It is clearly illustrated in Figure 8b that the outcomes of the present study are superior when compared with the literature

on similar domains, such as that of Wang et al. [27], Tang [28], Mohammed et al. [29], Eiamsa-ard et al. [30], Promvonge [31], and Chang et al. [32].

6. Conclusions

A computational study on HT and PD in a square-channel SWH with the insertion of semi-arc-shaped ribs was presented. As the working fluid, water was utilized, and the Re ranged from 4000 to 25,000. The present geometry encompassed semi-arc-shaped ribs with pitch ratios of 1.0, 1.5, and 2.0 and rib height ratios of 0.5, 0.4, and 0.25.

From the above computational study, the following conclusions may be drawn:

1. The insertion of novel-shaped ribs increases the Nusselt number by creating swirl flow in the flow field and enhancing the convective HT, and eventually, this leads to an augmentation of the overall heat transfer coefficient and results in an increased Nusselt number.
2. With an increase in the semi-arc-shaped rib height, the heat transfer rate increases, and at the same time, the friction factor is also increased significantly.
3. A decrease in the semi-arc-shaped rib pitch leads to enhancements in the heat transfer. However, more enhancement is noted when the rib height ratio is highest and the pitch ratio is lowest.
4. The Colburn j-factor and Bejan number were also presented, and the outcome is promising.
5. The thermal performance factor remains higher than unity for all the configurations investigated in the present numerical investigation. A pitch ratio of 1.0 and height ratio of 0.5 show the highest performance. The enhanced geometry is promising and may be implemented in the HVAC sector.

Some practical guidelines for optimizing the performance of novel arc-shaped rib inserts in a solar water heater are as follows:

1. Arc-shaped rib pitch ratio: Choose a pitch ratio that is optimal for the specific flow conditions. A higher pitch ratio can increase turbulence, but a pitch ratio that is too high can also cause excessive pressure drop.
2. Arc-shaped rib height ratio: The height of the rib can affect the amount of turbulence generated, with large rib heights generally causing more turbulence. One should choose a rib height that balances the desired level of turbulence with the pressure drop acceptable for the given system.
3. Rib material: The material of the rib can affect the heat transfer and corrosion resistance of the system. One should consider using a material with good thermal conductivity and resistance to corrosion for a specific application.
4. Flow rate: The flow rate through the system can affect the heat transfer and turbulence generated by the novel arc-shaped rib insert. One should choose a flow rate that balances the desired level of heat transfer with the pressure drop acceptable for the given system.

Author Contributions: Conceptualization, B.S. and S.B.; methodology, B.S. and S.B.; software, B.S. and S.B.; validation, B.S. and S.B.; formal analysis, B.S. and S.B.; investigation, B.S. and S.B.; resources, B.S. and S.B.; data curation, B.S. and S.B.; writing—original draft preparation B.S. and S.B.; writing—review and editing, B.S. and S.B.; visualization, B.S. and S.B.; supervision, B.S. and S.B.; project administration, B.S.; funding acquisition, B.S. All authors have read and agreed to the published version of the manuscript.

Funding: This work was supported by the Deanship of Scientific Research, Vice Presidency for Graduate Studies and Scientific Research, King Faisal University, Saudi Arabia (Grant No. 2413).

Data Availability Statement: The data that support the findings of this study are available from the corresponding author upon reasonable request.

Acknowledgments: Authors appreciate support by the Deanship of Scientific Research, Vice Presidency for Graduate Studies and Scientific Research, King Faisal University, Saudi Arabia (Grant No. 2413).

Conflicts of Interest: The authors declare no conflict of interest.

References

1. Gui, N.G.J.; Stanley, C.; Nguyen, N.-T.; Rosengarten, G. Ferrofluids for heat transfer enhancement under an external magnetic field. *Int. J. Heat Mass Transf.* **2018**, *123*, 110–121. [CrossRef]
2. Bhattacharyya, S.; Vishwakarma, D.K.; Goel, V.; Chamoli, S.; Issakhov, A.; Meyer, J.P. Thermodynamics and heat transfer study of a circular tube embedded with novel perforated angular-cut alternate segmental baffles. *J. Therm. Anal. Calorim.* **2021**, *145*, 1445–1465. [CrossRef]
3. Bhattacharyya, S.; Vishwakarma, D.K.; Srinivasan, A.; Soni, M.K.; Goel, V.; Sharifpur, M.; Ahmadi, M.H.; Issakhov, A.; Meyer, J. Thermal performance enhancement in heat exchangers using active and passive techniques: A detailed review. *J. Therm. Anal. Calorim.* **2022**, *147*, 9229–9281. [CrossRef]
4. Bezaatpour, M.; Goharkhah, M. Effect of magnetic field on the hydrodynamic and heat transfer of magnetite ferrofluid flow in a porous fin heat sink. *J. Magn. Magn. Mater.* **2019**, *476*, 506–515. [CrossRef]
5. Bhattacharyya, S.; Sharma, A.K.; Vishwakarma, D.K.; Paul, A.R. Thermo-hydraulic performance of magnetic baffles for removal of concentrated heat fluxes in a heated mini channel. *Appl. Therm. Eng.* **2022**, *216*, 118992. [CrossRef]
6. Bhattacharyya, S.; Vishwakarma, D.K.; Roy, S.; Biswas, R.; Ardekani, M.M. Applications of Heat Transfer Enhancement Techniques: A State-of-the-Art Review. In *Inverse Heat Conduction and Heat Exchangers*; IntechOpen: London, UK, 2020. [CrossRef]
7. Gawande, V.B.; Dhoble, A.; Zodpe, D.; Chamoli, S. Experimental and CFD investigation of convection heat transfer in solar air heater with reverse L-shaped ribs. *Sol. Energy* **2016**, *131*, 275–295. [CrossRef]
8. Deo, N.S.; Chander, S.; Saini, J. Performance analysis of solar air heater duct roughened with multigap V-down ribs combined with staggered ribs. *Renew. Energy* **2016**, *91*, 484–500. [CrossRef]
9. Zhang, C.; Wang, Z.; Kang, J. Flow and Heat Transfer in a High-Aspect-Ratio Rib-Roughed Cooling Channel with Longitudinal Intersecting Ribs. *J. Appl. Mech. Tech. Phys.* **2018**, *59*, 679–686. [CrossRef]
10. Ngo, T.T.; Phu, N.M. Computational fluid dynamics analysis of the heat transfer and pressure drop of solar air heater with conic-curve profile ribs. *J. Therm. Anal. Calorim.* **2020**, *139*, 3235–3246. [CrossRef]
11. Singh, P.; Ekkad, S. Experimental study of heat transfer augmentation in a two-pass channel featuring V-shaped ribs and cylindrical dimples. *Appl. Therm. Eng.* **2017**, *116*, 205–216. [CrossRef]
12. Yang, W.; Xue, S.; He, Y.; Li, W. Experimental study on the heat transfer characteristics of high blockage ribs channel. *Exp. Therm. Fluid Sci.* **2017**, *83*, 248–259. [CrossRef]
13. Alfarawi, S.; Abdel-Moneim, S.; Bodalal, A. Experimental investigations of heat transfer enhancement from rectangular duct roughened by hybrid ribs. *Int. J. Therm. Sci.* **2017**, *118*, 123–138. [CrossRef]
14. Tanda, G. Performance of solar air heater ducts with different types of ribs on the absorber plate. *Energy* **2011**, *36*, 6651–6660. [CrossRef]
15. Kumar, R.; Goel, V.; Singh, P.; Saxena, A.; Kashyap, A.S.; Rai, A. Performance evaluation and optimization of solar assisted air heater with discrete multiple arc shaped ribs. *J. Energy Storage* **2019**, *26*, 100978. [CrossRef]
16. Hans, V.; Gill, R.; Singh, S. Heat transfer and friction factor correlations for a solar air heater duct roughened artificially with broken arc ribs. *Exp. Therm. Fluid Sci.* **2017**, *80*, 77–89. [CrossRef]
17. Promvonge, P. Thermal performance in square-duct heat exchanger with quadruple V-finned twisted tapes. *Appl. Therm. Eng.* **2015**, *91*, 298–307. [CrossRef]
18. Mokkapati, V.; Lin, C.-S. Numerical study of an exhaust heat recovery system using corrugated tube heat exchanger with twisted tape inserts. *Int. Commun. Heat Mass Transf.* **2014**, *57*, 53–64. [CrossRef]
19. Abraham, S.; Vedula, R.P. Heat transfer and pressure drop measurements in a square cross-section converging channel with V and W rib turbulators. *Exp. Therm. Fluid Sci.* **2016**, *70*, 208–219. [CrossRef]
20. Chung, H.; Park, J.S.; Park, S.; Choi, S.M.; Rhee, D.-H.; Cho, H.H. Augmented heat transfer with intersecting rib in rectangular channels having different aspect ratios. *Int. J. Heat Mass Transf.* **2015**, *88*, 357–367. [CrossRef]
21. Liu, J.; Hussain, S.; Wang, W.; Xie, G.; Sundén, B. Experimental and numerical investigations of heat transfer and fluid flow in a rectangular channel with perforated ribs. *Int. Commun. Heat Mass Transf.* **2021**, *121*, 105083. [CrossRef]
22. Bhattacharyya, S.; Chattopadhyay, H.; Benim, A.C. Computational investigation of heat transfer enhancement by alternating inclined ribs in tubular heat exchanger. *Prog. Comput. Fluid Dyn. Int. J.* **2017**, *17*, 390. [CrossRef]
23. Bhattacharyya, S.; Benim, A.C.; Bennacer, R.; Dey, K. Influence of Broken Twisted Tape on Heat Transfer Performance in Novel Axial Corrugated Tubes: Experimental and Numerical Study. *Heat Transf. Eng.* **2021**, *43*, 437–462. [CrossRef]
24. Bhattacharyya, S.; Bashir, A.I.; Dey, K.; Sarkar, R. Effect of novel short-length wavy-tape turbulators on fluid flow and heat transfer: Experimental study. *Exp. Heat Transf.* **2020**, *33*, 335–354. [CrossRef]
25. Huminic, G.; Huminic, A. The heat transfer performances and entropy generation analysis of hybrid nanofluids in a flattened tube. *Int. J. Heat Mass Transf.* **2018**, *119*, 813–827. [CrossRef]
26. Bejan, A. A Study of Entropy Generation in Fundamental Convective Heat Transfer. *J. Heat Transf.* **1979**, *101*, 718–725. [CrossRef]
27. Wang, W.; Zhang, Y.; Li, B.; Li, Y. Numerical investigation of tube-side fully developed turbulent flow and heat transfer in outward corrugated tubes. *Int. J. Heat Mass Transf.* **2018**, *116*, 115–126. [CrossRef]

28. Tang, X.; Dai, X.; Zhu, D. Experimental and numerical investigation of convective heat transfer and fluid flow in twisted spiral tube. *Int. J. Heat Mass Transf.* **2015**, *90*, 523–541. [CrossRef]
29. Mohammed, H.A.; Abbas, A.K.; Sheriff, J. Influence of geometrical parameters and forced convective heat transfer in transversely corrugated circular tubes. *Int. Commun. Heat Mass Transf.* **2013**, *44*, 116–126. [CrossRef]
30. Eiamsa-Ard, S.; Rattanawong, S.; Promvonge, P. Turbulent convection in round tube equipped with propeller type swirl generators. *Int. Commun. Heat Mass Transf.* **2009**, *36*, 357–364. [CrossRef]
31. Promvonge, P. Thermal performance in circular tube fitted with coiled square wires. *Energy Convers. Manag.* **2008**, *49*, 980–987. [CrossRef]
32. Chang, S.W.; Yang, T.L.; Liou, J.S. Heat transfer and pressure drop in tube with broken twisted tape insert. *Exp. Therm. Fluid Sci.* **2007**, *32*, 489–501. [CrossRef]